

This is a repository copy of *Ferromagnetism in two-dimensional CrTe₂epitaxial films down to a few atomic layers*.

White Rose Research Online URL for this paper:

<https://eprints.whiterose.ac.uk/id/eprint/173595/>

Version: Published Version

Article:

Sun, Yizhe, Yan, Pengfei, Ning, Jiai et al. (11 more authors) (2021) Ferromagnetism in two-dimensional CrTe₂epitaxial films down to a few atomic layers. RSC Advances. 035138. ISSN: 2046-2069

<https://doi.org/10.1063/5.0041531>

Reuse

This article is distributed under the terms of the Creative Commons Attribution (CC BY) licence. This licence allows you to distribute, remix, tweak, and build upon the work, even commercially, as long as you credit the authors for the original work. More information and the full terms of the licence here:

<https://creativecommons.org/licenses/>

Takedown

If you consider content in White Rose Research Online to be in breach of UK law, please notify us by emailing eprints@whiterose.ac.uk including the URL of the record and the reason for the withdrawal request.

Ferromagnetism in two-dimensional CrTe₂ epitaxial films down to a few atomic layers

F

Cite as: AIP Advances **11**, 035138 (2021); <https://doi.org/10.1063/5.0041531>

Submitted: 30 January 2021 . Accepted: 16 February 2021 . Published Online: 23 March 2021

Yizhe Sun, Pengfei Yan, Jiai Ning, Xiaoqian Zhang, Yafei Zhao, Qinwu Gao, Moorthi Kanagaraj, Kunpeng Zhang, Jingjing Li,  Xianyang Lu, Yu Yan, Yao Li, Yongbing Xu, and  Liang He

COLLECTIONS

Paper published as part of the special topic on [Chemical Physics](#), [Energy, Fluids and Plasmas](#), [Materials Science](#) and [Mathematical Physics](#)

F

This paper was selected as Featured



View Online



Export Citation



CrossMark

ARTICLES YOU MAY BE INTERESTED IN

[Enhancing magneto-optic effects in two-dimensional magnets by thin-film interference](#)

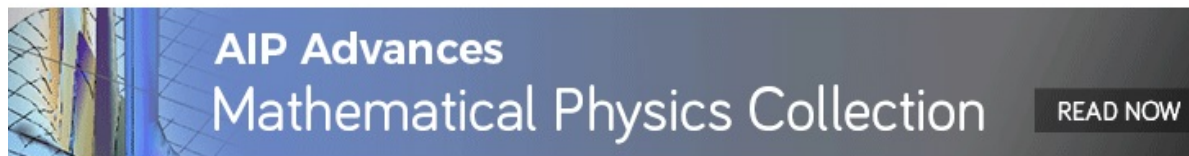
AIP Advances **11**, 035132 (2021); <https://doi.org/10.1063/5.0040262>

[Two-dimensional van der Waals spinterfaces and magnetic-interfaces](#)

Applied Physics Reviews **7**, 011303 (2020); <https://doi.org/10.1063/1.5112171>

[Cleavable magnetic materials from van der Waals layered transition metal halides and chalcogenides](#)

Journal of Applied Physics **128**, 110901 (2020); <https://doi.org/10.1063/5.0023729>





Ferromagnetism in two-dimensional CrTe₂ epitaxial films down to a few atomic layers

Cite as: AIP Advances 11, 035138 (2021); doi: 10.1063/5.0041531

Submitted: 30 January 2021 • Accepted: 16 February 2021 •

Published Online: 23 March 2021



Yizhe Sun,¹ Pengfei Yan,¹ Jiai Ning,¹ Xiaoqian Zhang,¹ Yafei Zhao,¹ Qinwu Gao,¹ Moorthi Kanagaraj,¹ Kunpeng Zhang,² Jingjing Li,³ Xianyang Lu,¹  Yu Yan,¹ Yao Li,^{1,4} Yongbing Xu,^{1,2,4} and Liang He^{1,4,a)} 

AFFILIATIONS

¹National Laboratory of Solid State Microstructures and Jiangsu Provincial Key Laboratory of Advanced Photonic and Electronic Materials, School of Electronic Science and Engineering, Nanjing University, Nanjing 210093, China

²Nanjing-York Joint Center of Spintronics and NanoEngineering and Department of Physics, The University of York, York YO105DD, United Kingdom

³School of Art and Design, Chuzhou University, Chuzhou 239000, China

⁴Collaborative Innovation Center of Advanced Microstructures, Nanjing University, Nanjing 210093, China

^{a)}Author to whom correspondence should be addressed: heliang@nju.edu.cn

ABSTRACT

Two-dimensional (2D) van der Waals ferromagnetic materials have attracted intense attention due to their potential impact on both fundamental and applied research studies. Recently, a new 2D ferromagnet CrTe₂, prepared by mechanical exfoliation or chemical vapor deposition, has gained interest due to its novel magnetic properties. In this work, high quality CrTe₂ epitaxial thin films were prepared on GaAs (111)B substrates using solid source molecular beam epitaxy, with the thickness varying from 35 to 4 monolayers (MLs). The magnetic easy axis of all the films is oriented along the c-axis. A Curie temperature of 205 K is found in the 35 ML CrTe₂ film, measured by the temperature-dependent anomalous Hall resistance (R_{AHE}). Importantly, even when the film thickness decreases to 4 MLs, a robust out-of-plane ferromagnetism with a Curie temperature of 191 K has been demonstrated. This finding could pave the way for investigating the fundamental studies in 2D ferromagnetism and has great significance in device applications.

© 2021 Author(s). All article content, except where otherwise noted, is licensed under a Creative Commons Attribution (CC BY) license (<http://creativecommons.org/licenses/by/4.0/>). <https://doi.org/10.1063/5.0041531>

Atomically thin two-dimensional (2D) van der Waals (vdW) materials have attracted extensive attention¹ owing to their remarkable properties in diverse experimental fields, such as electronics,^{2,3} optoelectronics,^{4–6} magnetism,⁷ thermoelectrics,⁸ and spintronic devices.⁹ Among these, intrinsic 2D magnetic materials, such as CrI₃,¹⁰ Fe₃GeTe₂,^{11,12} and Cr₂Ge₂Te₆,¹³ have aroused great interest not only due to their fascinating magnetic properties in the 2D limit but also for opening new avenues for applications in spintronics.^{13–15} Recently, a new 2D ferromagnetic material CrTe₂ has been found.^{16,17} Freitas *et al.* reported that they had synthesized the metastable compound 1T-CrTe₂ for the first time.¹⁶ Purbawati *et al.* reported thin CrTe₂ flakes with a T_c above room temperature.¹⁸ Sun *et al.* found that the ferromagnetism could hold above room temperature in a metallic phase of 1T-CrTe₂ down to the ultra-thin limit.¹⁹ However, all of the reported CrTe₂ are prepared in bulk forms, and the devices are made by mechanical exfoliation and stacking techniques.^{12,19–21} The size and thickness of 2D materials obtained by

exfoliation are uncontrolled, which prevents them being applied in actual production. Thus, the preparation of the large-scale samples with high quality is of great significance.

In this work, a series of CrTe₂ thin films with various thicknesses from 35 to 4 monolayers (MLs) were epitaxially grown on high resistivity ($\approx 10 \text{ M}\Omega \text{ cm}$) GaAs (111)B substrates using molecular beam epitaxy (MBE). The base pressure of the growth chamber is below 2×10^{-10} Torr. The GaAs (111)B substrates were cleaned under a standard procedure before being loaded into the chamber.²² Then, the substrates were annealed at 580 °C in the growth chamber until the streak patterns appeared as monitored by the real-time RHEED,²³ as shown in Fig. 1(b). High-purity Cr (99.999%) and Te (99.9999%) were evaporated by conventional effusion cells. During the growth, the Cr effusion cell was kept at 1180 °C and the Te effusion cell was kept at 255 °C to keep the flux ratio of Cr/Te at 1/20 to maintain a Te-rich environment. The GaAs (111)B substrates were set at 265 °C during the growth for all the samples.

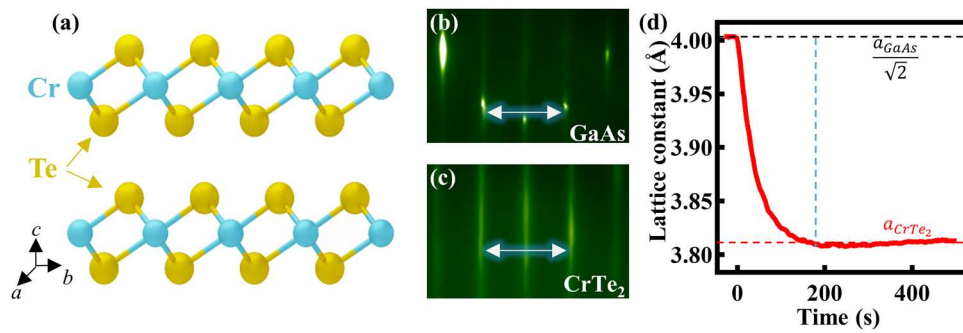


FIG. 1. (a) Schematics of the crystal structure of CrTe_2 . The RHEED patterns of the GaAs (111)B substrate (b) and a CrTe_2 thin film (c), respectively. The double-headed arrows between the two first order stripes represent the d -spacing, which is inversely proportional to the in-plane lattice constant. (d) The time evolution of the lattice constant of the film during growth. The black horizontal and red dashed lines indicate the lattice constant of the GaAs (111)B substrate and CrTe_2 film, respectively. The blue dashed line shows the finishing time of the first ML.

Figure 1(a) presents the crystalline structure of the CrTe_2 compound. They crystallize in the space group of $p\bar{3}m1$, with the layered structures stacked by the Te–Cr–Te sandwich layers along the c axis,¹⁸ while between the layers, the interactions are mainly of the van der Waals type.²⁴ Figures 1(b) and 1(c) show representative RHEED patterns of the GaAs (111)B substrate and the CrTe_2 , respectively. Sharp streaky patterns were observed after growth, which indicates the flat surface morphology of the films. The double-headed arrows between the two first order stripes represent the d -spacing,²⁵ which is inversely proportional to the in-plane lattice constant. For GaAs (111)B, the atoms are close-packed in the (111) plane, which makes its in-plane lattice constant to be $a_{\text{GaAs}}/\sqrt{2}$ of ~ 4.0 Å, as shown by the black dashed line in Fig. 1(d). From this, the lattice constant of the films can be extracted to be 3.81 Å, which is very close to the theoretical value of 3.79 Å,^{18,26} as shown by the red dashed line in Fig. 1(d). Figure 1(d) illustrates the evolution of the lattice constant of CrTe_2 film during growth. Soon after the beginning of the growth, the lattice constant of the film decreases from the GaAs substrates and reaches CrTe_2 after the first layer, as indicated by the blue dashed line. This suggests that the films have completely released the strain from the substrate after the growth of the first layer, which is consistent with the van der Waals epitaxial growth mode.²⁷

Figure 2(a) shows a typical atomic force microscopy (AFM) (NT-MDT, INTEGRA SPECTRA II, Probe aperture size ~ 100 nm) image of an as-grown CrTe_2 film. Hexagonal terraces can be observed with a typical size of ~ 200 nm, reflecting the hexagonal crystal structure inside the (0001) plane.²⁸ Figure 2(b) displays the height profile of the dashed line in Fig. 2(a). The height is equal to ~ 6.1 Å, consistent with a CrTe_2 ML thickness.^{16,26} The phase purity and crystal structure of the CrTe_2 thin film have been identified by x-ray diffraction (Bruker D8 Discover single crystal diffractometer, $\lambda = 1.5406$ Å) and the spectra are shown in Fig. 2(c). Compared with the Joint Committee on Powder Diffraction Standards (JCPDS) data of CrTe_2 , the film has been found to exhibit rhombohedral crystal geometry with no other detectable phases.²⁴ The lattice parameter c was calculated as 6.144 Å according to the position of the XRD peaks, which is consistent with the value of 6.166 Å by the theoretical calculation.^{19,24}

After growth, the samples are patterned into standard Hall bar devices using Ion Beam Etching (IBE) with Ar gas. The magnetic properties of the samples were examined by the magneto-transport measurements inside an Oxford instruments' cryogenic system (TeslatronPT), as shown in Fig. 3(a). A Keithley 6221 AC/DC current source was used to apply an AC of 1 μA with a frequency of 13 Hz. Lock-in amplifier SR830 was employed to obtain the

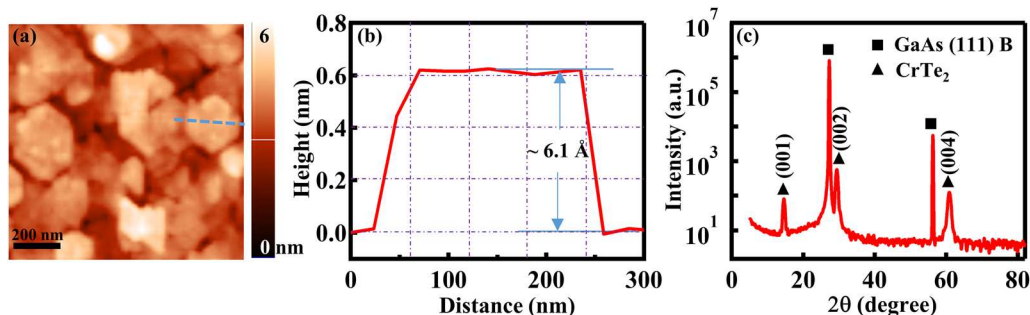


FIG. 2. (a) A typical AFM image of an as-grown CrTe_2 film. (b) The height profile along the dashed line in (a) demonstrates that the terrace height is ~ 6.1 Å, about one CrTe_2 layer. (c) XRD pattern of a 35 ML CrTe_2 thin film.

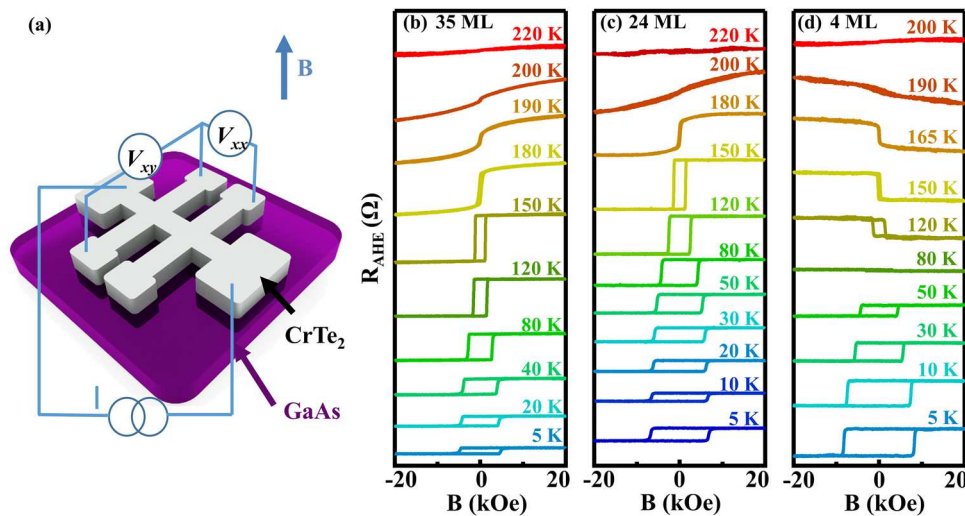


FIG. 3. (a) A schematic diagram of the CrTe₂ (white) on a highly resistive GaAs (111)B (purple) Hall bar device with the measurement setup. Anomalous Hall resistance, $R_{AHE} = R_{xy} - R_0 H$, of the 35 (b), 24 (c), and 4 ML (d) CrTe₂ film vs magnetic field at various temperatures.

longitudinal and transverse voltage signals, while the magnetic field up to 2 T was scanned back and forth perpendicular to the sample surface.

Generally, there is a close correlation between magnetism and transport in magnetic materials, and the anomalous Hall effect (AHE) is utilized to demonstrate the prevailing ferromagnetism. The Hall resistance (R_{xy}) follows an empirical relation²⁹ $R_{xy} = R_0 H + R_A M(H)$, where the first term is the ordinary Hall effect and the second is the AHE with respective coefficients R_0 and R_A .³⁰ Here, R_0 is the ordinary Hall coefficient and is solely connected to the carrier density, and R_A is proportional to the longitudinal resistance R_{xx} or R_{xx}^{-2} depending on the dominant extrinsic scattering mechanisms.³¹

By subtracting the linear ordinary Hall component $R_0 H$, the anomalous Hall data $R_{AHE} = R_{xy} - R_0 H$ of 35, 24, and 4 ML CrTe₂ films were plotted at different temperatures in Figs. 3(b)–3(d),

respectively. For the 35 ML CrTe₂ film, a square hysteresis loop can be observed at low temperatures, suggesting its ferromagnetism and the out-of-plane easy axis. As the temperature rises, the saturated R_{AHE} first increases and reaches the maximum at about 150 K, then decreases, and finally disappears around 200 K, as shown in Fig. 4(a). The coercive field (H_c) decreases and eventually vanished around 200 K. Similar behaviors are also observed in the 24 ML sample, as shown in Fig. 3(c).

For the 4 ML CrTe₂ film, as the temperature increases, the saturated R_{AHE} first decreases from positive to negative at 80 K, reaches its minimum at 150 K, then increases again, and finally disappears at around 190 K. This strange temperature dependent saturated R_{AHE} , only found at very thin samples, may be associated with the change of their intrinsic anomalous Hall coefficient, which is related to their Berry curvatures.³² On the other hand, its coercive field (H_c)

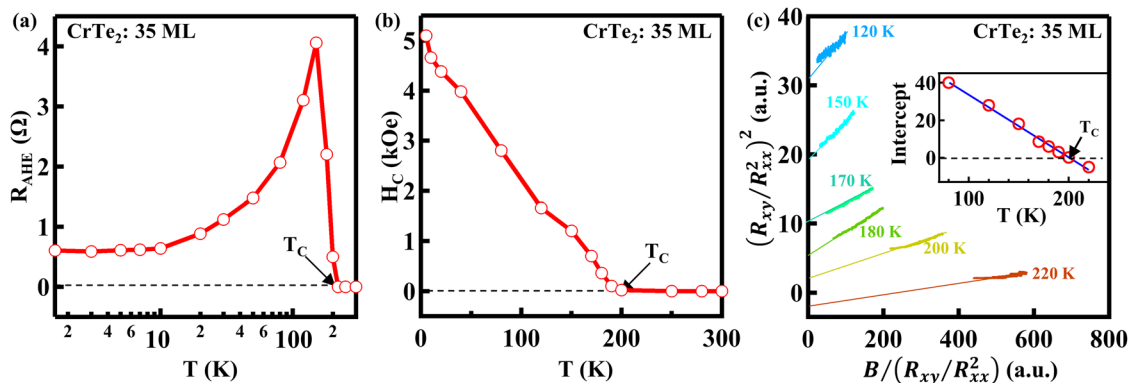


FIG. 4. (a) The saturated R_{AHE} vs temperature of the 35 ML CrTe₂. The Curie temperature can be determined as ~ 202 K. (b) The H_c vs temperature of the 35 ML CrTe₂. The Curie temperature can be determined as ~ 203 K. (c) Arrott-plot using anomalous Hall data at temperatures from 120 K to 220 K. The lines in different colors represent the linear fits at high fields where the magnetization is saturated. (Inset) The intercepts in the y-axis vs temperatures. The linear fit gives the Curie temperature of 204.6 ± 0.8 K.

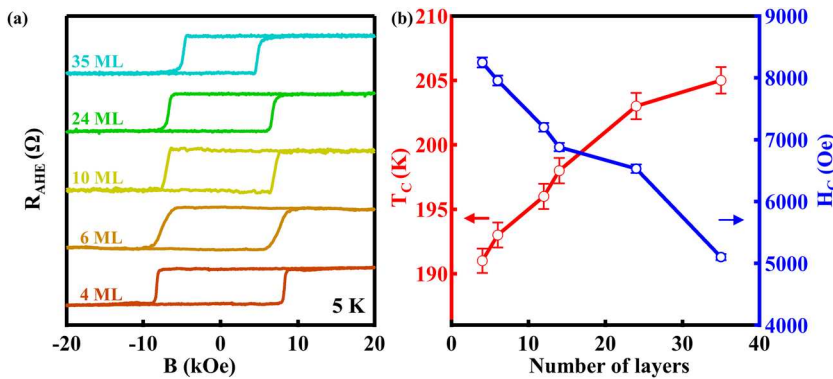


FIG. 5. (a) Magnetic field dependent anomalous Hall effect (R_{AHE}) with different CrTe_2 thicknesses. (b) The evolution of the Curie temperature T_C (red) and the coercive field H_C (blue) at 5 K vs CrTe_2 thicknesses. The Curie temperature raises with the increasing film thicknesses, while the coercivity correspondingly decreases.

decreases monotonically with the increased temperature and reaches zero at 191 K.

The temperature dependent saturated R_{AHE} of the 35 ML CrTe_2 is plotted in Fig. 4(a), and the Curie temperature of 202 K can be determined as it reaches zero.³³ Figure 4(b) shows the H_C as a function of temperature. As the temperature increases, H_C drops and reaches zero at 203 K. In addition, the method of the Arrott-plot has been adopted to further confirm the ferromagnetic transition.³⁴ Here, we take the assumption of side jump mechanism at high fields and use the ratio of (R_{xy}/R_{xx}^2) to estimate the magnetization M .^{35,36} Thus, the Arrott-plot can be plotted as $(R_{xy}/R_{xx}^2)^2$ against $B/(R_{xy}/R_{xx}^2)$, where B is magnetic induction,³⁷ as shown in Fig. 4(c). It is well known that the intercept on the y-axis of the extrapolated line at high field is positive for the ferromagnetic state and negative for the paramagnetic state.³⁸ When the intercept goes to zero, the Curie temperature T_C of 204.6 ± 0.8 K can be determined,³⁹ as shown in the inset of Fig. 4(c). All three methods presented here give a consistent T_C of ~ 205 K for the 35 ML CrTe_2 films. The T_C for all other prepared samples has been determined similarly, as shown in Fig. 5(b). It decreases from 205 to 191 K, as the film thickness decreases from 35 to 4 MLs.

Figure 5(a) presents the R_{AHE} of various CrTe_2 thin films at 5 K. All the samples exhibit similar square hysteresis loops, demonstrating strong ferromagnetism with an out-of-plane easy axis even for the 4 ML sample.⁴⁰ As shown in Fig. 5(b), the H_C increases as the sample thickness decreases and reaches 8200 Oe at 4 ML. This increase in coercivity is probably due to the increase in shape anisotropy originating from magnetostatic or dipole interactions.⁴¹

In summary, a series of CrTe_2 thin films with various thicknesses have been synthesized by MBE. All the films show strong ferromagnetism with an out-of-plane easy axis. More importantly, as the film thickness decreases from 35 to 4 ML, the Curie temperature decreases only slightly from 205 to 191 K, while the coercive field (H_C) increases from 5120 to 8200 Oe. With distinct magnetic properties, large area CrTe_2 thin films grown by MBE are promising for stacking with other 2D materials and suitable for all van der Waals material electronic devices.

See the [supplementary material](#) for RHEED patterns of the CrTe_2 thin films with different thicknesses, RHEED intensity oscillations during growth, x-ray diffraction methods to calculate the lattice parameter c , and R_{AHE} of all the CrTe_2 films vs magnetic field at various temperatures.

This work was supported by the National Key Research and Development Program of China (Grant Nos. 2016YFA0300803 and 2017YFA0206304), the National Natural Science Foundation of China (Grant Nos. 61474061, 61674079, 61974061, and 61805116), the Natural Science Foundation of Jiangsu Province of China (Grant Nos. BK20180056 and BK20200307), and the China Postdoctoral Science Foundation, China (Grant No. 2019M661787).

DATA AVAILABILITY

The data that support the findings of this study are available from the corresponding author upon reasonable request.

REFERENCES

- W. Han, R. K. Kawakami, M. Gmitra, and J. Fabian, *Nat. Nanotechnol.* **9**(10), 794–807 (2014).
- Z. Lin, Y. Liu, U. Halim, M. Ding, Y. Liu, Y. Wang, C. Jia, P. Chen, X. Duan, and C. Wang, F. Song, M. Li, C. Wan, Y. Huang, and X. Duan, *Nature* **562**(7726), 254–258 (2018).
- D. Akinwande, N. Petrone, and J. Hone, *Nat. Commun.* **5**(1), 5678 (2014).
- Q. H. Wang, K. Kalantar-Zadeh, A. Kis, J. N. Coleman, and M. S. Strano, *Nat. Nanotechnol.* **7**(11), 699–712 (2012).
- K. F. Mak and J. Shan, *Nat. Photonics* **10**(4), 216–226 (2016).
- B. W. H. Baugher, H. O. H. Churchill, Y. Yang, and P. Jarillo-Herrero, *Nat. Nanotechnol.* **9**, 262 (2014).
- V. O. Yazyev, *Rep. Prog. Phys.* **73**(5), 056501 (2010).
- G. Z. Magda, P. Vancsó, Z. Osváth, P. Nemes-Incze, and L. Biró, *Nature* **514**, 608 (2014).
- D. Zhong, K. L. Seyler, X. Linpeng, R. Cheng, N. Sivadas, B. Huang, E. Schmidgall, T. Taniguchi, K. Watanabe, and M. A. McGuire, *Sci. Adv.* **3**(5), e1603113 (2017).
- S. Jiang, L. Li, Z. Wang, K. F. Mak, and J. Shan, *Nat. Nanotechnol.* **13**, 549 (2018).
- Y. Deng, Y. Yu, Y. Song, J. Zhang, N. Z. Wang, Z. Sun, Y. Yi, Y. Z. Wu, S. Wu, and J. Zhu, *Nature* **563**, 94 (2018).
- Z. Fei, B. Huang, P. Malinowski, W. Wang, T. Song, J. Sanchez, W. Yao, D. Xiao, X. Zhu, A. F. May, W. Wu, D. H. Cobden, J.-H. Chu, and X. Xu, *Nat. Mater.* **17**(9), 778–782 (2018).
- M. Mogi, A. Tsukazaki, Y. Kaneko, R. Yoshimi, K. S. Takahashi, M. Kawasaki, and Y. Tokura, *APL Mater.* **6**(9), 091104 (2018).
- H. Ohno, D. Chiba, F. Matsukura, T. Omiya, E. Abe, T. Dietl, Y. Ohno, and K. Ohtani, *Nature* **408**, 944 (2000).
- B. Huang, G. Clark, E. Navarro-Moratalla, D. R. Klein, R. Cheng, K. L. Seyler, D. Zhong, E. Schmidgall, M. A. McGuire, and D. H. Cobden, *Nature* **546**, 270 (2017).
- D. C. Freitas, R. Weht, A. Sulpice, G. Remenyi, and P. Strobel, F. Gay, J. Marcus, M. Núñez-Regueiro, *J. Phys.: Condens. Matter* **27**(17), 176002 (2015).

- ¹⁷K. Lasek, P. M. Coelho, K. Zberecki, Y. Xin, and M. Batzill, *ACS Nano* **14**, 8473 (2020).
- ¹⁸A. Purbawati, J. Coraux, J. Vogel, A. Hadj-Azzem and N. Rougemaille, *ACS Appl. Mater. Interfaces* **12**, 30702 (2020).
- ¹⁹X. Sun, W. Li, X. Wang, Q. Sui, T. Zhang, Z. Wang, L. Liu, D. Li, S. Feng, S. Zhong, H. Wang, V. Bouchiat, M. Nunez Regueiro, N. Rougemaille, J. Coraux, A. Purbawati, A. Hadj-Azzem, Z. Wang, B. Dong, X. Wu, T. Yang, G. Yu, B. Wang, Z. Han, X. Han, and Z. Zhang, *Nano Res.* **13**, 3358–3363 (2020).
- ²⁰D. R. Klein, D. Macneill, J. L. Lado, D. Soriano, E. Navarro-Moratalla, K. Watanabe, T. Taniguchi, S. Manni, P. Canfield, J. Fernández-Rossier, and P. Jarillo-Herrero, *Science* **360**(6394), 1218–1222 (2018).
- ²¹C. Gong, L. Li, Z. Li, H. Ji, A. Stern, Y. Xia, T. Cao, W. Bao, C. Wang, Y. Wang, Z. Q. Qiu, R. J. Cava, S. G. Louie, J. Xia, and X. Zhang, *Nature* **546**(7657), 265 (2017).
- ²²Y. Sun, M. Kanagaraj, Q. Gao, Y. Zhao, J. Ning, K. Zhang, X. Lu, L. He, and Y. Xu, *Chin. Phys. Lett.* **37**(7), 077501 (2020).
- ²³L. He, F. Xiu, Y. Wang, A. V. Fedorov, G. Huang, X. Kou, M. Lang, W. P. Beyermann, J. Zou, and K. L. Wang, *J. Appl. Phys.* **109**, 103702 (2011).
- ²⁴A. O. Fumega, J. S. Phillips, and V. Pardo, *J. Phys. Chem. C* **124**, 21047 (2020).
- ²⁵L. He, X. Kou, and K. L. Wang, *Phys. Status Solidi RRL* **7**, 50–63 (2013).
- ²⁶H. Y. Lv, W. J. Lu, D. F. Shao, Y. Liu, and Y. P. Sun, *Phys. Rev. B* **92**, 214419 (2015).
- ²⁷L. He, X. Kou, M. Lang, E. S. Choi, Y. Jiang, T. Nie, W. Jiang, Y. Fan, Y. Wang, F. Xiu, and K. L. Wang, *Sci. Rep.* **3**, 3406 (2013).
- ²⁸K. Wang, Y. Liu, W. Wang, N. Meyer, L. H. Bao, L. He, M. R. Lang, Z. G. Chen, X. Y. Che, K. Post, J. Zou, D. N. Basov, K. L. Wang, and F. Xiu, *Appl. Phys. Lett.* **103**(3), 031605–031604 (2013).
- ²⁹X. F. Kou, W. J. Jiang, M. R. Lang, F. X. Xiu, L. He, Y. Wang, Y. Wang, X. X. Yu, A. V. Fedorov, P. Zhang, and K. L. Wang, *J. Appl. Phys.* **112**(6), 063912 (2012).
- ³⁰F. Tsui, L. He, L. Ma, A. Tkachuk, Y. S. Chu, K. Nakajima, and T. Chikyow, *Phys. Rev. Lett.* **91**(17), 177203 (2003).
- ³¹N. Nagaosa, J. Sinova, S. Onoda, A. H. MacDonald and N. P. Ong, *Rev. Mod. Phys.* **82**(2), 1539–1592 (2010).
- ³²W. Liu, D. West, L. He, Y. Xu, J. Liu, K. Wang, Y. Wang, G. van der Laan, R. Zhang, S. Zhang, and K. L. Wang, *ACS Nano* **9**(10), 10237–10243 (2015).
- ³³F. Cui, X. Zhao, J. Xu, B. Tang, Q. Shang, J. Shi, Y. Huan, J. Liao, Q. Chen, and Y. Hou, *Adv. Mater.* **32**(4), 1905896 (2020).
- ³⁴D. Zhang, A. Richardella, D. W. Rench, S. Y. Xu, and N. Samarth, *Phys. Rev. B* **86**(20), 205127 (2012).
- ³⁵A. Arrott, *Phys. Rev.* **108**(6), 1394–1396 (1957).
- ³⁶F. Matsukura, H. Ohno, A. Shen, and Y. Sugawara, *Phys. Rev. B* **57**(4), R2037 (1998).
- ³⁷I. Stouchnov, S. W. E. Riester, H. J. Trodahl, N. Setter, A. W. Rushforth, K. W. Edmonds, R. P. Campion, C. T. Foxon, B. L. Gallagher, and T. Jungwirth, *Nat. Mater.* **7**(6), 464–467 (2008).
- ³⁸J. Ning, Y. Zhao, Z. Chen, Y. Sun, Q. Gao, Y. Chen, M. Kanagaraj, J. Zhang, and L. He, *J. Phys. D: Appl. Phys.* **53**(50), 505001 (2020).
- ³⁹L. Bao, W. Wang, N. Meyer, Y. Liu, C. Zhang, K. Wang, P. Ai, and F. Xiu, *Sci. Rep.* **3**, 2391 (2013).
- ⁴⁰H. U. Jingshi and T. F. Rosenbaum, *Nat. Mater.* **7**(9), 697–700 (2008).
- ⁴¹Y. Fujisawa, M. Pardo-Almanza, J. Garland, K. Yamagami, X. Zhu, X. Chen, K. Araki, T. Takeda, M. Kobayashi, Y. Takeda, C. H. Hsu, F. C. Chuang, R. Laskowski, K. H. Khoo, A. Soumyanarayanan, and Y. Okada, *Phys. Rev. Mater.* **4**(11), 114001 (2020).